A musculoskeletal full-body simulation of cross-country skiing

L. Joakim Holmberg and A. M. Lund

Original Publication:

L. Joakim Holmberg and A. M. Lund, A musculoskeletal full-body simulation of cross-country skiing, 2008, Proc. IMechE Vol. 222 Part P: J. Sports Engineering and Technology, (222), 1, 11-22.
http://dx.doi.org/10.1243/17543371JSET10

A musculoskeletal full-body simulation of cross-country skiing

L J Holmberg[1,2]* and **A M Lund**[3]
[1]Swedish Winter Sports Research Centre, Mid Sweden University, Östersund, Sweden
[2]Division of Mechanics, Linköping University, Linköping, Sweden
[3]Department of Engineering, Physics, and Mathematics, Mid Sweden University, Östersund, Sweden

The manuscript was received on 13 December 2007 and was accepted after revision for publication on 10 April 2008.

DOI: 10.1243/17543371JSET10

Abstract: This paper presents a measurement-driven, musculoskeletal, full-body simulation model for biomechanical analysis of the double-poling (DP) technique in cross-country skiing. DP is a fast and powerful full-body movement; therefore, it is interesting to examine whether inverse dynamics using static optimization is working for a musculoskeletal full-body model with high accelerations, a large range of motion, and realistic loads. An experiment was carried out to measure motion and pole force of a skier on a double-poling ergometer. Using the measurement data, a simulation model was implemented in the AnyBody Modeling System (AnyBody Technology A/S, Denmark). Experimental results of motion and pole force from the DP ergometer, and also simulation results of relative muscle force profiles, are presented. These results agree with results found in literature when the kinematics and external kinetics are similar. Consequently, it should be possible to use computer simulations of this type for cross-country skiing simulations. With a simulation model, it is possible to perform optimization studies and to ask and answer 'what if' questions. Solutions to such problems are not easy to obtain by traditional testing alone.

Keywords: biomechanics, double poling, ergometer, inverse dynamics

1 INTRODUCTION

Popular goals for using biomechanics in sports are:

1. improvement of performance by technique, equipment, or training;
2. injury prevention and rehabilitation [**1**].

To achieve these goals, it is common to experimentally measure athletes' motion, forces, and electromyography (EMG) and draw conclusions directly from the experimental results alone. In contrast, it is also possible to increase the understanding of a specific sport by theoretical reasoning using classical mechanics, for example in rowing [**2**]. A more advanced method for integrating mechanics into the analysis is to make a mechanical model of the athlete and the equipment used, followed by a simulation of this model. The greatest advantage with simulations is the possibility of answering 'what if' questions, such as 'If a cross-country skier used a greater abduction of the upper arm at pole plant, what would happen with the load distribution between muscles that work as arm extensors in the poling phase?'

The spectrum of human-body models for performing biomechanical simulations in sports is vast. They range from a single or a few rigid bodies without muscles in two dimensions (2D) to large, linked systems of rigid bodies with advanced muscle mechanics in three dimensions (3D) [**3–6**]. Examples in alpine skiing include Gerritsen *et al.* [**7**] and Casolo *et al.* [**8**], and, in ski-jumping, Ettema and Bråten [**9**].

In cross-country skiing, biomechanics has not been studied extensively [**10**]; mostly, experimental measurements of motion, force, and EMG have been performed [**11–18**]. To the best of the authors' knowledge, there have only been three simulation studies in cross-country skiing [**19–21**]; two of them were musculoskeletal upper-body models [**19**, **20**] and one a musculoskeletal full-body model [**21**].

**Corresponding author: Swedish Winter Sports Research Centre, Mid Sweden University, Östersund, 83125, Sweden. email: joakim.holmberg@miun.se*

They were, however, not capable of handling the external loads to full extent.

Cross-country skiing is a complex, full-body motion with interaction between equipment (skis and poles) and snow. The motion is relatively fast compared to, for instance, gait, which is commonly simulated [**22**, **23**]. Because the whole body is contributing in all cross-country sub-techniques, and in double poling (DP) [**12**], a cross-country simulation for gross movements must use a full-body model. DP is an important sub-technique in cross-country skiing [**17**], and also the best one to begin with for cross-country skiing simulations, because the DP motion takes place mainly in the sagittal plane. It is basically 2D, and therefore enables both easier capturing of the motion and easier implementation.

For musculoskeletal simulations, there are mainly two methods: dynamic and static optimization. The dynamic method, forward approach, solves one optimization problem for the complete movement cycle. The method of static optimization solves a different optimization problem at every time step (instant) during the movement. This is the critical difference between the methods, and also the reason why dynamic optimization needs more computing power compared to the static optimization [**23**]. Inverse dynamics can be viewed as when a prescribed motion drives the body model, and the internal forces needed to generate this motion are sought. An inverse dynamics-simulation model for cross-country DP needs a full-body model, which means a large number of muscles and degrees of freedom. Therefore, static optimization is preferable. Nevertheless, choosing static optimization rules out the possibility of including muscle activation dynamics. This can be negative because DP is a rather fast motion that possibly needs activation dynamics to yield good results [**24**].

The aims of this study are:

1. to create a stable measurement-driven musculoskeletal, full-body, 3D simulation model of cross-country DP that can handle realistic external loads;
2. to examine whether it is possible to use inverse dynamics and static optimization for musculoskeletal simulation models with high accelerations and a large range of motion, i.e. the DP movement.

2 METHOD

2.1 Implementation summary

A simulation model consisting of a body model and boundary conditions was implemented in the AnyBody modelling system (version 3.0, AnyBody Technology A/S, Aalborg, Denmark). This software is a general modelling system for musculoskeletal inverse dynamics [**25**]. The body model consisted of muscles, bones, and joints. Because motion and external forces were used as input to the simulation, an experiment was carried out to obtain these boundary conditions. In the experiment, a skier was videotaped while skiing on a DP ergometer equipped with load cells at the pole tips. The output from an AnyBody simulation is muscle forces. Those may be used for comparison of simulation results with literature. Simulations were performed on an IBM T40p Laptop with 1 GB RAM running at 1600 MHz.

2.2 Inverse dynamics and static optimization of musculoskeletal systems

The approach shown here, similar to that of Nikravesh [**26**], is to use a full set of Cartesian co-ordinates for each body in the system and then to apply the Newton–Euler equations of motion. The spatial positions of the bodies relative to an inertial reference frame are described by $\boldsymbol{q}$. Kinematic constraints describe the effect of joints in a multibody system, and, in the case of inverse dynamics, also the driving constraints that specify the prescribed motion. The time-dependent kinematic constraint equations are.

$$\Phi \equiv \Phi(\boldsymbol{q}, t) = \mathbf{0} \tag{1}$$

The derivatives are

$$\Phi_q \dot{\boldsymbol{q}} + \Phi_t = \mathbf{0} \tag{2}$$

and

$$\Phi_q \ddot{\boldsymbol{q}} + (\Phi_q \dot{\boldsymbol{q}})_q \dot{\boldsymbol{q}} + 2\Phi_{qt} \dot{\boldsymbol{q}} + \Phi_{tt} = \mathbf{0} \tag{3}$$

In equations (2) and (3), $\dot{\boldsymbol{q}}$ is the velocity vector and $\ddot{\boldsymbol{q}}$ is the acceleration vector for the bodies in the system, respectively; the matrix Φ_q is the constraint Jacobian. The subscript 'q' is used for partial derivatives with respect to the spatial positions, and the subscript 't' is used for partial derivatives with respect to time.

The Newton–Euler equations of motion for a spatial system of constrained bodies can be written in compact form, suitable for inverse dynamics, as

$$\boldsymbol{g}^c + \boldsymbol{g}^u = \mathbf{M}\dot{\boldsymbol{h}} + \boldsymbol{b} - \boldsymbol{g}^k \tag{4}$$

where $\boldsymbol{g}^c$ contains the constraint (reaction) forces between connecting bodies, and $\boldsymbol{g}^u$ contains the unknown forces of the actuators; $\mathbf{M}$ is the system mass matrix; $\boldsymbol{h}$ is the system velocity vector; $\boldsymbol{b}$ contains fictitious forces, such as Coriolis; $\boldsymbol{g}^k$ contains the known applied forces, such as gravity. Only the left-hand side of equation (4) contains unknowns, and therefore it is possible to solve the equation for $\boldsymbol{g}^c$ and $\boldsymbol{g}^u$.

In the case of musculoskeletal inverse dynamics, muscles are the actuators. Mechanically speaking, however, the human body has more muscles than necessary to perform many motions. In reality, this excess of muscles and the force sharing between them are taken care of by the central nervous system. Prilutsky and Zatsiorsky [**24**] state that humans are able to repeat movements with great precision, and that relative muscle force profiles are very similar for different people performing the same movement. Therefore, it is believed that the central nervous system controls the muscle forces based on some unknown but rational criterion.

In a numerical model of the human body, it is possible to use optimization to solve the force-sharing problem. A number of optimization criteria have been suggested in literature [**27**]. One possibility is a minimum fatigue criterion that distributes the collaborative muscle forces in such a way that the maximum relative muscle force is as small as possible, a so-called minimum–maximum criterion [**28**]. In this study, using AnyBody and the minimum–maximum criterion, the force-sharing problem is formulated as

$$\underset{\beta, f}{\text{minimize}}\ \beta \tag{5}$$

subject to

$$\frac{f_i^m}{N_i} \leqslant \beta, \quad i \in \{1, \ldots, n\} \tag{6}$$

$$f_i^m \geqslant 0, \quad i \in \{1, \ldots, n\} \tag{7}$$

$$\mathrm{C}\boldsymbol{f} = \boldsymbol{d} \tag{8}$$

Here, f_i^m is individual muscle force, N_i is a normalizing function with maximum available strength of each individual muscle, and n is the number of muscles. The constraint equations of (7) simply state that muscles can only pull, not push. To facilitate the representation of each individual muscle in the equations of motion, they are reformulated in the constraint equation (8) as compared to equation (4). C is a geometry- and kinematics-dependant coefficient matrix for the unknown muscle and constraint forces in $\boldsymbol{f}$, while $\boldsymbol{d}$ is simply the right-hand side of equation (4). This formulation of the force-sharing problem, using equations (5)–(8), leads to a linear optimization problem.

The minimum–maximum criterion has some inherent problems because it only cares about the maximal relative force of the muscles, and muscles with sub-maximal force production may be left undetermined. This calls for an iterative scheme where determined muscles and their force contribution are eliminated from equation (8) in every iteration until all muscles are determined. For an explanation of the software implementation of this approach, see [**29**].

To conclude, the approach to inverse dynamics of musculoskeletal systems shown in this paper involves these three basic steps:

1. kinematic analysis (equations (1), (2), and (3));
2. the evaluation of the properties of the multibody system (N_i, C, and d);
3. the solution of the force-sharing problem (equations (5)–(8)).

2.3 Body model

A publicly available 3D full-body model from AnyScript Model Repository version 6.1 (The AnyBody Project, Aalborg University, Aalborg, Denmark) served as a base for the implementation. All anthropometric properties (and their origins) are listed in the body model files found at the repository webpage (currently, http://www.anybody.aau.dk/repository). The body model had roughly the same limb lengths and inertia properties as the participating skier. This body model consisted of rigid bodies constrained by joints and muscles, which worked as force actuators. All major body parts were represented in the body model. Limb-inertia properties are distributed to the rigid body segments (bones). Effects from wobbly masses of soft tissues are neglected. One major simplification that affects this type of motion is the fixed position of scapula relative to the trunk. Joints are also simplified and most of them are modelled as either revolute, universal, or spherical joints. The spine had a special joint set-up that facilitates spinal motion. There was no muscle dynamics included. As mentioned in the introduction, activation dynamics is ruled out by the method. Contraction dynamics was not used due to lack of relevant data. All muscles were modelled with a constant available force and without tendons or other passive element properties. This rules out stretch-shortening effects on the muscle force. Most muscles were divided into several pieces because the muscles are geometrically modelled as linear elements spanning from the origin point to the insertion point, sometimes via other points and surfaces to enable wrapping around joints and other bony objects.

In order to make it possible to drive the 3D full-body model with captured 2D motion, a 2D human dummy was created and added to the body model. A pair of poles was also added to the body model for easier implementation of measured pole forces. In total, the biomechanical system used in the simulations consisted of 464 individual muscle elements and 64 rigid bodies. For visualization purposes, a pair of skis was added – see Fig. 1.

Fig. 1 Body model used in the simulation together with the 2D dummy

2.4 Boundary conditions

An experiment was carried out to obtain the motion and pole forces. A trained, male skier was videotaped using a DP ergometer (Erg), specifically designed for DP testing, and also used in [**30**] – see Fig. 2.

This apparatus is a modified rowing ergometer. The skier stands on a podium above a slide rail. The ergometer has poles attached to a metal bar mounted on a slide wagon, which connects to a fixed pulley system by means of a cord. The pulley is connected to a chain that drives the air friction-braked flywheel by means of a cogwheel. In contrast to Holmberg and Nilsson [**30**], the load cells (U9B 1 kN, HBM, Germany) are installed at the pole tips to measure the axial pole force directly. The load cells are connected to a measurement system (Spider8 and catman Express, version 4; HBM, Germany) for real-time display and the recording of pole forces.

The forces were measured at 100 Hz during a series of 30 s measurements. Simultaneously, the motion in the sagittal plane was captured at 25 Hz using a digital video camera (DCR-TRV50E, Sony Corporation, Japan). By studying individual video frames and the pole force curve, the time for a complete poling cycle was determined to about 1.4 s. By manual inspection, one representative poling cycle was chosen from a series of consistent cycles. Fifteen frames in this cycle were used to extract (Dartfish, version 4.0, Dartfish, Switzerland) selected joint angles (ankle, knee, hip, shoulder, elbow, wrist, and hand-to-pole), spine curvature, and the position of the pole. Spine curvature was measured by the angle between the pelvis (an approximate line between the greater trochanter and the iliac crest) and the upper part of thorax (an approximate line between the vertebrae T1–T3). All measurements were of the right side of the skier.

Fig. 2 Skier on the double poling ergometer

Collected data from the measurement were applied to the body model as boundary conditions, thereby creating a simulation model. The feet were held fixed in the simulations. Driven dummy angles were ankle, knee, hip, shoulder, elbow, wrist, and hand-to-pole. The 3D body model was then constrained to 'follow' the 2D dummy in a parasagittal plane at certain joints centres and 2D motion was projected up to 3D motion – see Fig. 1, in which the 2D dummy is located in the sagittal plane. In addition to this, the curvature of the spine and the pole inclination of the 3D body model were driven. The pole force from the measurements were applied to the poles of the body model so that the muscles of the body model needed to create the same force in the poles.

To use the measured kinematics and pole forces in the simulation, they must be smoothed to fit together in the simulation and also to prevent unrealistic segment accelerations. Therefore, all measured motion data were smoothed with a Bézier interpolation spline.

3 RESULTS

In the following result presentation, pole inclination, and joint angles are defined as shown in Fig. 3

Measurements from the DP ergometer showed that the cycle time (CT) for a complete poling cycle was 1.4 s. The poling-phase time (PT) of one complete poling cycle is defined as the time when the pole tips are moving backwards on the DP ergometer. Relative poling-phase (PTrel), defined as PT/CT, was 50 per cent. Peak pole force (PF) is the maximum pole force that was registered during the poling cycle, and the time to peak pole force (TPF) is the time it takes to reach PF from the start of the poling cycle. The relative time to peak pole force (TPFrel), defined as TPF/PT, was 50 per cent. Figure 4 shows measured pole force and selected joint angles during a complete poling cycle on the DP ergometer. The result curves were interpolated with a straight line between the data points.

Selected simulation kinematics from the 3D body model during a complete poling cycle are shown in Fig. 5. Maximum angular acceleration of some representative body model joints were 12 rad/s^2 (elbow), 29 rad/s^2 (hip), and 2 rad/s^2 (knee).

Simulation kinetics, i.e. relative muscle force of selected muscles and pole force, are shown in Fig. 6. Relative muscle force is defined as 'carried force' by the muscle divided by the 'maximum available force' of the muscle. Relative muscle force levels are defined as LOW (2 per cent $<$ relative muscle force $\leqslant$ 18 per cent), MEDIUM (18 per cent $<$ relative muscle force $\leqslant$ 57 per cent), and HIGH (57 per cent

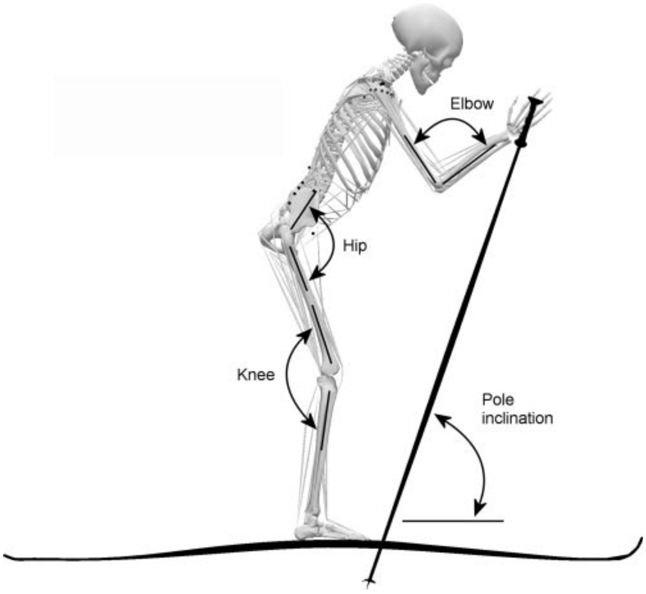

Fig. 3 Definition of pole inclination and joint angles used in the result presentation

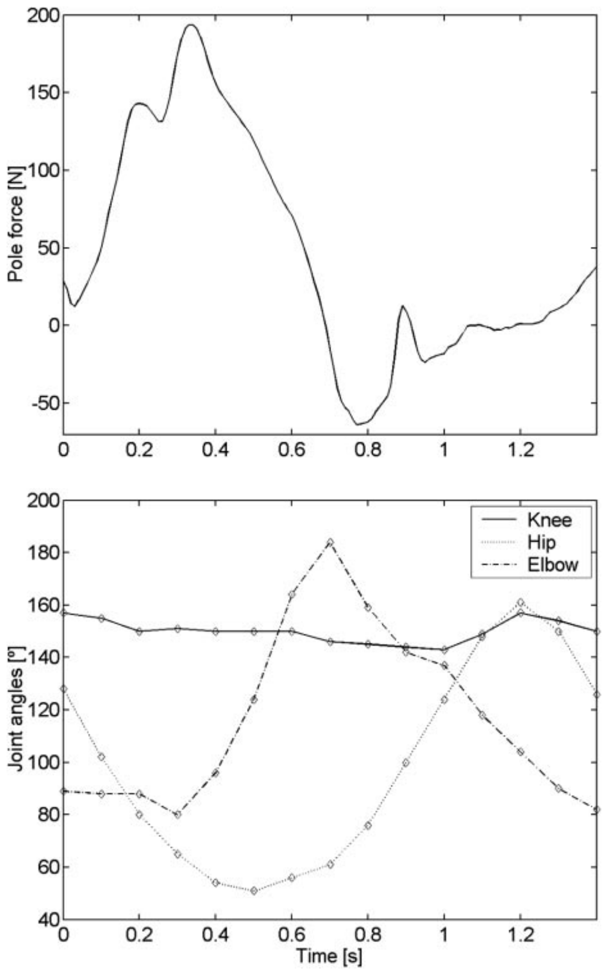

Fig. 4 Experimental results from the double poling ergometer: pole force and selected joint angles of the right side

< relative muscle force ⩽ 100 per cent). This level definition is consistent with EMG activity levels from Holmberg et al. [**11**]. Presented muscles are biceps brachii long head (BIC); latissimus dorsi (LD); levator scapulae (LS); pectoralis major (PMa); rhomboid major and minor (RHO); teres major (TMa); trapezius, the scapular part (TRA_s) and the clavicular part (TRA_c); triceps brachii long head (TRI); rectus femoris (RF); biceps femoris long head (BFLH); biceps femoris short head (BFSH); iliopsoas (ILI); external abdominal oblique (OE); internal abdominal oblique (OI); and rectus abdominis (RA).

4 DISCUSSION

The main findings in this study show: the first relatively stable measurement-driven musculoskeletal full-body simulation of cross-country skiing with realistic loads, and the possibility to use inverse dynamics and static optimization for a full-body simulation with large accelerations and a large range of motion.

The reason for this study was not to make a validation study, but rather to take the first steps toward creating a stable simulation model for cross-country skiing. For a validation study, EMG data, kinematics, and pole force should be measured in the same study. Also, it is possible that the simulation model needs a greater level of detail concerning muscle activation dynamics. Therefore, another objective in this study was to examine whether inverse dynamics using static optimization is working for a full-body model with large accelerations and a large range of motion. However, no joint acceleration results (or any other measure of 'fastness or powerfulness') have been found in literature to enable a clear comparison to other movements in that aspect. Muscle forces that are calculated without muscle contraction dynamics and activation dynamics can not be directly compared to EMG measurements, but no previous muscle force measurements or calculations for this kind of movement have been found in literature. Therefore, a comparison of simulated normalized muscle force profiles and EMG data has been carried out. Both give an indication of when a certain muscle is producing force during a movement. Care has been taken to account for the lack of muscle dynamics in the simulation. The comparison of simulation results and EMG data in literature showed some similarities and some differences (a more detailed comparison follows, below). Although it is impossible at this stage to specify exactly where all the differences originate from, it is important, when working with simulations, to remember that a model is always a model and that it will always include

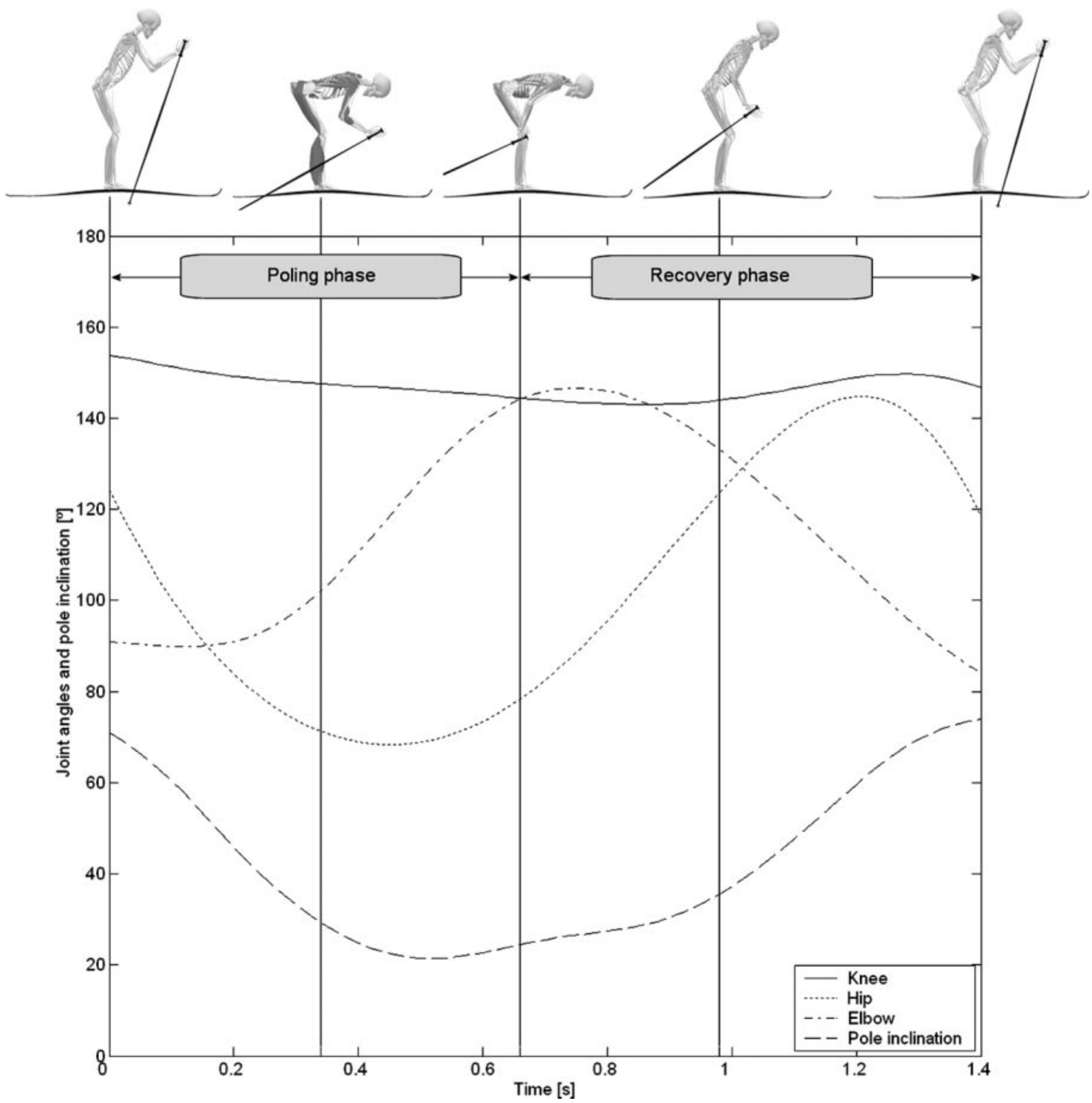

Fig. 5 Simulation kinematics, selected joint angles, and pole inclination

uncertainties. Furthermore, as mentioned by Vaughan [**31**], one disadvantage of simulations is the difficulty to validate the model and the method. However, even with unknown accuracy of the biomechanical simulation, a model can provide new understanding and new possibilities. It is also worth to mention that this kind of simulation (musculoskeletal, full-body model using inverse dynamics and static optimization) can be performed on an ordinary personal computer (PC).

In the implementation of the model in this study, there have been some stability problems. It remains unknown if the problems occurred because of the large model, the existence of mechanical closed loops in the model, or the uncertainties of the input (body model and boundary conditions).

Kinematics and pole force are shown in Fig. 4 for a skier working on this type of Erg. This is the first time such a presentation has been made. It also shows that there are differences between the results of this ergometer study and the results of roller ski studies [**11**, **18**].

This simulation of DP is performed from measurements of a skier working on an Erg. However, EMG data exists from roller skiing, and it would have been better for the comparison if the simulation were also performed on roller skiing. Full-body musculoskeletal simulations in 3D with many muscles are computationally hard, because of both mechanical and numerical stability. The reason for choosing an Erg is that the kinematics and kinetics become more symmetrical than for

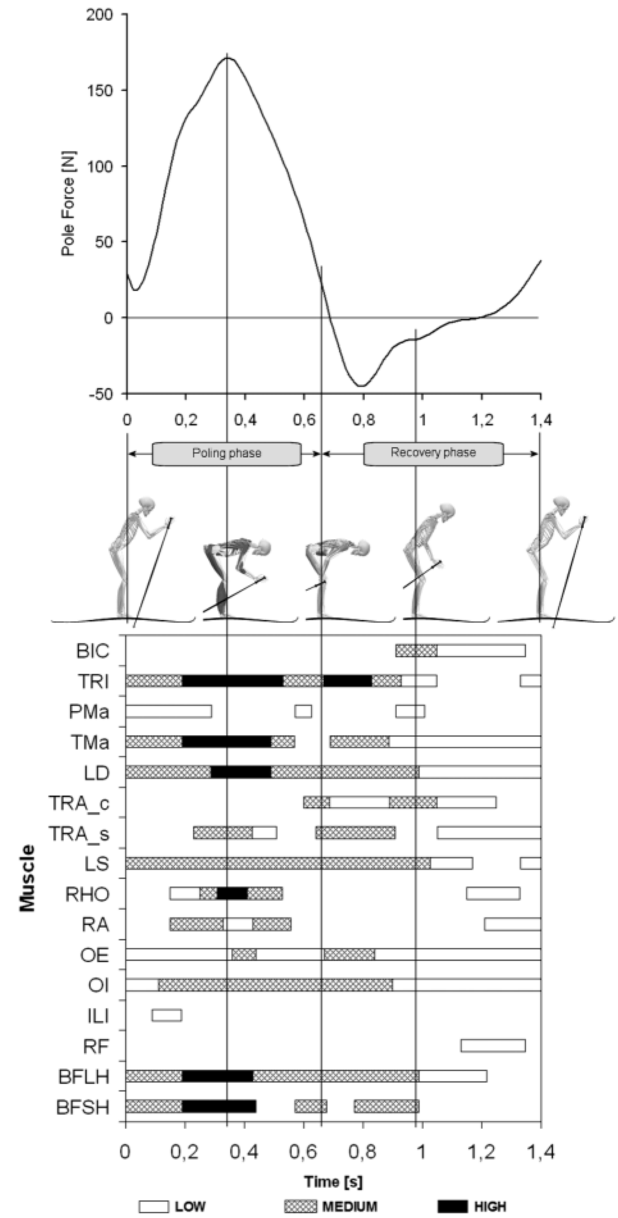

Fig. 6 Simulation kinetics, pole force, and relative muscle force of selected muscles. Relative muscle force is defined as 'carried force' by the muscle divided by the 'maximum available force' of the muscle. Relative muscle force levels are defined as LOW, MEDIUM, and HIGH. Presented muscles are: biceps brachii long head (BIC); latissimus dorsi (LD); levator scapulae (LS); pectoralis major (PMa); rhomboid major and minor (RHO); teres major (TMa); trapezius, the scapular part (TRA_s) and the clavicular part (TRA_c); triceps brachii long head (TRI); rectus femoris (RF); biceps femoris caput longum (BFLH); biceps femoris short head (BFSH); iliopsoas (ILI); external abdominal oblique (OE); internal abdominal oblique (OI); rectus abdominis (RA)

roller skiing, and hence better mechanical stability is achieved. It also makes sense to ground the body model at the feet, thereby achieving better numerical stability. Because measured kinematics are from parasagittal planes, it is assumed that right and left side are symmetrical and spinal motion is restricted to flexion and extension. The applied boundary conditions, in the simulation model did not include reactions forces under the feet (skis), but, as the feet were grounded in space in the model, the reaction forces between the feet and the Erg podium were computed by the simulation. Also, reaction forces from the poles were applied, which makes the system kinematically determinate. Adding reaction force from the feet would have resulted in an overdetermined system and probably dynamically inconsistent due to measurement uncertainties.

In Fig. 4, some of the measured kinematic quantities are shown. Spine curvature, shoulder angle, wrist angle, and hand-to-pole angle were also measured, but these are not presented as there are no directly comparable data in the literature. To use the measured kinematics and pole forces in the simulation, the data had to be smoothed. The obvious reason is that the low sampling frequency of the kinematics would yield unrealistic accelerations. Additionally, the measured pole force had two distinct peaks, but there was no kinematics to 'support' them. This is because the kinematics was sampled as a much lower frequency than the pole force, and the kinematics and pole force did not 'fit' unless the pole force was also smoothed. Smoothed kinematics and pole force are shown in Figs 5 and 6. This smoothing of the input can be done in several ways; here, a Bézier interpolation (within the software) was chosen.

It can be observed in Fig. 6 that the poling force is still positive at the end of the poling-phase, and not zero as it should be. This is a result of the smoothing, and therefore strange relative muscle forces may appear in the beginning of the return phase. The poling force could have been rescaled to fit the end of the poling cycle; this was not done because we did not want to perturb the data additionally.

When comparing the relative muscle force profiles from the simulation with EMG data from literature, it is important to first compare the differences in recorded kinematics and pole force. There are two sources that have reported EMG data: Stöggl *et al.* [**18**] and Holmberg *et al.* [**11**]. Both are studies made of roller skiing (Rski). Stöggl *et al.* have measured kinematics and pole forces for six elite skiers working on a slope with 3° inclination. In their study, CT was 1.01 s, PTrel was 50 per cent, and TPFrel was 30 per cent. Holmberg *et al.* measured kinematics and pole forces for 11 elite skiers working on a tread-mill. In their study, CT was 1.13 s, PTrel was 27 per cent, and TPFrel was 30 per cent. Differences for PTrel and TPFrel between the two studies can originate both from different inclination and strategy (technique) chosen by the skiers.

In this study, CT was 1.4 s, PTrel was 50 per cent, and TPFrel was 50 per cent. For this study, CT was longer than in the Rski studies of Stöggl *et al.* and Holmberg *et al.*, PTrel was equal to the study made by Stöggl *et al.*, and larger compared to Holmberg *et al.* TPFrel was larger compared to Holmberg *et al.* and equal compared to Stöggl *et al.* One reason for the difference between DP on an Erg and on Rski is that the pole tips in the Erg were fixated to a wagon sliding on rails. This affects the motion of the poles and, therefore, the whole kinematics and kinetics. The poles first push the wagon backwards and then try to pull it forward and upward (which is not possible), hence the negative pole force in the recovery phase. The system of poles and wagon is more inert than the 'free' poles in Rski. The more inert system for Erg compared to Rski affects both CT, PTrel, and TPFrel. The increased inertia decreases the accelerations of the poles according to Newton's second law, and therefore CT, PTrel, and TPFrel are prolonged. This explains why the workload for the Erg was more continuous than for Rski. The prolongation of TPFrel also originates from the impossibility of moving the poles from the rails. When the poles are 'free', higher acceleration in the direction of the poles is achieved at the pole plant, and PF is reached faster. Another difference is that the Erg kinematics does not result in the same amount of stretch-shortening of the muscle. Even if it would, the muscle model used in the simulation can not take stretch-shortening effects on the muscle force into account.

The muscles in the simulation model have a maximum available force. There are differences between the model's muscle force and the skiers' maximum voluntary contraction in the Rski. This means that it is hard to compare simulated relative muscle force and EMG activation levels. The possible comparison of the simulation results and EMG data in literature is relative to when a muscle produces force (or indication of that it produces force), but care has to be taken due to the differences in timing because there was no muscle dynamics present in the simulation.

The simulation gives results for all muscles in the model. That is an advantage compared to experimental testing where it can be troublesome and perhaps impossible to measure everything. Mainly, muscles that can be compared to results in literature are presented, but also muscles considered important for poling but impossible to measure with surface EMG, for example ILI and OI – see Fig. 6. The wrist and the spine were areas where kinematics was measured roughly. Hence, muscles around the wrist and the dorsal of the pelvic bone and the spine are not presented. The foot was modelled as a rigid segment fixed to the ground, which is considered unrealistic. Therefore, muscles around the ankle joint are not presented either. Here, it is important to point out that all calculated muscle forces were reasonable in the sense that no single muscle element had to work harder than physically possible and there was still a unique solution to the load distribution.

With the insight on how Erg and Rski differ, it is meaningful to compare relative muscle force profiles from this simulation (Erg-Sim) shown in Fig. 6 and EMG results from Rski studies by Stöggl *et al.* [**18**] and Holmberg *et al.* [**11**]. Overall, the comparison demonstrates two important issues. Firstly, the largest total muscle work occurred around PF for all studies. The PF in Rski studies occurred earlier than in Erg-Sim, and the comparison of relative force profiles showed that many muscles in Rski studies were active earlier than in Erg-Sim. Secondly, the Erg-Sim results showed more muscle work in the recovery phase than the Rski studies. That is because the poles needed more applied force to be transported forward in the recovery phase.

For a closer comparison, the results can be divided into three groups: first, arms and shoulders, then trunk and hips, and, last, legs. The arms and shoulders include five muscles possible to compare: BIC, TRI, TMa, PMa, and LD. Work of BIC was similar in Rski and Erg-Sim in the recovery phase, although Erg-Sim showed higher relative muscle force. In Rski, BIC also worked during the poling phase, especially around the pole plant. TRI and TMa worked mainly around PF for both Rski and Erg-Sim. In Erg-Sim, TRI and TMa also worked hard in the first half of the recovery phase. PMa worked mainly before and at PF for Rski, and, for Erg-Sim, mainly before PF. For LD, maximum force was attained at PF. In Erg-Sim, it worked during the whole CT, while in Rski it was resting during the main part of the recovery phase.

The other presented muscles – RHO, LS, TRA_c, and TRA_s – were all affected by the fixed position of the scapula relative to the trunk during the motion. They are presented to show that they indeed did work. RHO clearly worked around PF.

In the trunk and hip region, there are four muscles presented: RA, OE, OI, and ILI. From Rski studies, EMG data are only presented for RA and OE, probably because the use of surface EMG in the Rski studies. Erg-Sim results and Rski EMG showed only vague similarities, but this region has more uncertain kinematic measures than other parts.

The leg muscles presented here are BFLH, RF, and BFSH. BFSH is not presented in Rski literature, and no comparison was possible. BFSH showed a similar force pattern as BFLH, but with some gaps of zero work. In Erg-Sim, BFLH worked during the poling-phase, and it continued to the middle of the recovery phase. Maximal force occurred at PF. For Rski, BFLH worked from around PF and a short time into the recovery phase. Rski and Erg-Sim were similar in the late poling-phase and in the beginning of the recovery phase. The work in RF was similar for Erg-Sim and Rski in the last part of the recovery phase. In Rski, RF also worked around pole plant.

The comparison of the results from the simulation and EMG data from literature showed some similarities and some differences. In the parts where the kinematics was more accurate, the force profiles showed more consistency. These areas were the legs, the arms, and the shoulder. For example, TRI and PMa were similar for all studies; RF and BIC were quite similar in Rski and Erg, except that they worked more around pole plant in Rski. RF and BIC worked as antagonists at the pole plant. In the Rski studies, there was a higher acceleration at pole plant, which resulted in higher force more quickly, and the antagonists needed to stabilize the motion more than in the Erg-Sim study.

In conclusion, the present study showed a measurement-driven, musculoskeletal, full-body simulation of DP in cross-country skiing. This is the first known simulation model of cross-country skiing of this complexity that is both relatively stable and can handle realistic loads. The input, the kinematics, and the pole force, as well as the output, the relative muscle force profiles, were compared to other studies of DP and showed similarities and differences both in input and output. Two central issues were observed:

1. most work occurred around PF for the Erg-Sim study as well as the Rski studies;
2. the muscles worked more in the recovery phase in the Erg-Sim study than in the Rski studies

Overall, simulation results indicate that it is possible to use inverse dynamics and static optimization for a full-body simulation with large accelerations and a large range of motion. Even though there are, and always will be, uncertainties, the authors believe these kind of simulations can add new knowledge to cross-country skiing.

ACKNOWLEDGEMENTS

Most of this work was carried out with financial support from the European Union. We would like to thank the Swedish Winter Sports Research Centre at Mid Sweden University in Östersund for providing us with laboratory resources. Finally, we would like to thank the participating skier.

REFERENCES

1 **McGinnis, P. M.** *Biomechanics of sport and exercise*, 2nd edition, 2005, (Human Kinetics, Champaign, IL).
2 **Baudouin, A.** and **Hawkins, D.** A biomechanical review of factors affecting rowing performance. *Br. J. Sports Med.*, 2002, **36**, 396–402.
3 **Yanai, T.** and **Hay, J. G.** Combinations of cycle rate and length for minimizing the muscle power requirement in human running. *J. Appl. Biomech.*, 2004, **20**, 57–70.
4 **Matsuo, T., Matsumoto, T., Mochizuki, Y., Yoshihiro, T.,** and **Saito, K.** Optimal shoulder abduction angles during baseball pitching from maximal wrist velocity and minimal kinetics viewpoints. *J. Appl. Biomech.*, 2002, **18**, 306–320.
5 **Hase, K., Kaya, M., Zavatsky, A. B.,** and **Halliday, S. E.** Musculoskeletal loads in ergometer rowing. *J. Appl. Biomech.*, 2004, **20**, 317–323.
6 **Raasch, C. C., Zajac, F. E., Ma, B.,** and **Levine, W. S.** Muscle coordination of maximum-speed pedaling. *J. Biomechanics*, 1997, **30**, 595–602.
7 **Gerritsen, K. G. M., Nachbauer, W.,** and **van den Bogert, A. J.** Computer simulation of landing movement

in downhill skiing: anterior cruciate ligament injuries. *J. Biomechanics*, 1996, **29**, 845–854.
8 **Casolo, F., Lorenzi, V., Vallatta, A.,** and **Zappa, B.** Simulation techniques applied to skiing mechanics. In *Science and Skiing I*, E. Müller, E. Kornexl, C. Raschner (Eds), 1997, pp. 116–130 (Chapman and Hall, Cambridge, UK).
9 **Ettema, G.** and **Bråten, S.** On the role of the location of centre of mass in ski jumping. In *Science and Nordic Skiing*, Linnamo, V., Komi, P.V. and Müller, E. (Eds), 2007, pp. 197–204 (Meyer and Meyer Sport, Oxford, UK).
10 **Lindinger, S.** Biomechanics in cross-country skiing – Methods and future research questions. In *Science and Nordic Skiing*, Linnamo, V., Komi, P.V. and Müller, E. (Eds), 2007, pp. 23–42 (Meyer and Meyer Sport, Oxford, UK).
11 **Holmberg, H.-C., Lindinger, S., Stöggl, T., Eitzlmair, E.,** and **Müller, E.** Biomechanical analysis of double poling in elite cross-country skiers. *Med. Sci. Sports Exerc.*, 2005, **37**, 807–818.
12 **Holmberg, H.-C., Lindinger, S., Stöggl, T., Björklund, G.,** and **Müller, E.** Contribution of the legs to double-poling performance in cross-country skiers. *Med. Sci. Sports Exerc.*, 2006, **38**, 1853–1860.
13 **Millet, G. Y., Hoffman, M. D., Candau, R. B.,** and **Clifford, P. S.** Poling forces during roller skiing: effects of grade. *Med. Sci. Sports Exerc.*, 1998, **30**, 1637–1644.
14 **Millet, G. Y., Hoffman, M. D., Candau, R. B.,** and **Clifford, P. S.** Poling forces during roller skiing: effects of technique and speed. *Med. Sci. Sports Exerc.*, 1998, **30**, 1645–1653.
15 **Nilsson, J., Tveit, P.,** and **Eikrehagen, O.** Effects of speed on temporal patterns in classical style and freestyle cross-country skiing. *Sports Biomech.*, 2004, **3**, 85–118.
16 **Nilsson, J., Jakobsen, V., Tveit, P.,** and **Eikrehagen, O.** Pole length and ground reaction forces during maximal double poling in skiing. *Sports Biomech.*, 2003, **2**, 227–236.
17 **Smith, G. A., Fewster, J. B.,** and **Braudt, S. M.** Double poling kinematics and performance in cross-country skiing. *J. Appl. Biomech.*, 1996, **12**, 88–103.
18 **Stöggl, T., Lindinger, S.,** and **Müller, E.** Biomechanical validation of a specific upper body training and testing drill in cross-country skiing. *Sports Biomech.*, 2006, **5**, 23–46.
19 **Holmberg, J.** and **Wagenius, P.** A biomechanical model of a double-poling skier. In International Society of Biomechanics XIXth Congress on *The human body in motion* CD Rom Abstracts and Proceedings, Milburn, P. (Ed.) University of Otago, Dunedin, New Zealand, 6–11 July 2003.
20 **Lund, A. M.** and **Holmberg, L. J.** Which are the antagonists to the pectoralis major muscle in 4th gear freestyle technique, cross-country skiing? In *Science and Nordic Skiing*, Linnamo, V., Komi, P.V., and Müller, E. (Eds) 2007, pp. 112–118 (Meyer and Meyer Sport, Oxford, UK).
21 **Holmberg, L. J.** and **Lund, A. M.** Using double-poling simulations to study the load distribution between teres major and latissimus dorsi. In *Science and Nordic Skiing*, Linnamo, V., Komi, P.V., and Müller, E. (Eds) 2007, pp. 81–89 (Meyer and Meyer Sport, Oxford, UK).
22 **Thelen, D. G.** and **Anderson, F. C.** Using computed muscle control to generate forward dynamic simulations of human walking from experimental data. *J. Biomechanics*, 2006, **39**, 1107–1115.
23 **Anderson, F. C.** and **Pandy, M. G.** Static and dynamic optimization solutions for gait are practically equivalent. *J. Biomechanics*, 2001, **34**, 153–161.
24 **Prilutsky, B. I.** and **Zatsiorsky, V. M.** Optimization-based models of muscle coordination. *Exerc. Sport Sci. Rev.*, 2002, **30**, 32–38.
25 **Damsgaard, M., Rasmussen, J., Christensen, S. T., Surma, E.,** and **de Zee, M.** Analysis of musculoskeletal systems in the AnyBody Modeling System. *Simulation Modelling Practice and Theory*, 2006, **14**, 1100–1111.
26 **Nikravesh, P. E.** *Computer-aided analysis of mechanical systems*, 1998, (Prentice-Hall, Eaglewood Cliffs, NJ).
27 **Tsirakos, D., Baltzopoulos, V.,** and **Bartlett, R.** Inverse optimization: functional and physiological considerations related to the force-sharing problem. *Critical Reviews in Biomedical Engineering*, 1997, **25**, 371–407.
28 **Rasmussen, J., Damsgaard, M.,** and **Voigt, M.** Muscle recruitment by the min/max criterion–a comparative numerical study. *J. Biomechanics*, 2001, **34**, 409–415.
29 **Damsgaard, M., Rasmussen, J.,** and **Christensen, S. T.** Inverse dynamics of musculo-skeletal systems using an efficient min/max muscle recruitment model. In Proceedings of DETC'01: *ASME 2001 Design Engineering Technical Conferences and Computers and Information in Engineering Conference*, Pittsburgh, Pennsylvania, 9–12 September 2001, paper DETC2001/VIB-21347.
30 **Holmberg, H. -C.** and **Nilsson, J.** Reliability and validity of a new double poling ergometer for cross-country skiers. *J. Sports Sciences*, 2007, **25**, 1–9.
31 **Vaughan, C. L.** Computer simulation of human motion in sports biomechanics. *Exerc. Sport Sci. Rev.*, 1984, **12**, 373–416.

APPENDIX

Notation

b	vector of fictitious forces, such as Coriolis
C	coefficient matrix for the unknown muscle and constraint forces
d	right-hand side of equation (4)
DP	double poling
EMG	electromyography
f	vector of unknown muscle and constraint forces
f_i^m	muscle force for muscle i
g^c	vector of constraint forces between connecting bodies
g^k	vector of known applied forces, such as gravity
g^u	vector of actuator forces
h	system velocity vector
M	system mass matrix
N_i	normalizing function with maximum available strength of muscle i

n number of muscles
q vector of spatial positions for bodies in the system
$\dot{\boldsymbol{q}}$ vector of velocities for bodies in the system
$\ddot{\boldsymbol{q}}$ vector of accelerations for bodies in the system
$_q$ subscript for partial derivatives with respect to spatial positions
t time
$_t$ subscript for partial derivatives with respect to time
β objective function of minimum/maximum formulation
Φ kinematic constraint equations
Φ_q constraint Jacobian matrix